



Design, synthesis, and biological evaluation of new raloxifene analogues of improved antagonist activity and endometrial safety

George Lambrinidis^{a,*}, Cedric Gouedard^b, Sotiria Stasinopoulou^b, Angeliki Angelopoulou^b, Vassiliki Ganou^b, Aggeliki K. Meligova^b, Dimitra J. Mitsiou^b, Panagiotis Marakos^a, Nicole Pouli^a, Emmanuel Mikros^{a,*}, Michael N. Alexis^{b,*}

^a Department of Pharmacy, National and Kapodistrian University of Athens, Panepistimiopolis Zografou, 15771 Athens, Greece

^b Institute of Chemical Biology, National Hellenic Research Foundation, 48, Vassileos Constantinou Avenue, 11635 Athens, Greece

ARTICLE INFO

Dedicated to the memory of Prof. George B. Foscolos.

Keywords:
Drug design
SERMs
Endometrial safety
Estrogen receptors
Hormones
Raloxifene

ABSTRACT

Raloxifene agonism of estrogen receptor (ER) in post-menopausal endometrium is not negligible. Based on a rational drug design workflow, we synthesized 14 analogues of raloxifene bearing a polar group in the aromatic ring of the basic side chain (BSC) and/or changes in the bulkiness of the BSC amino group. Analogues with a polar BSC aromatic ring and amino group substituents of increasing volume displayed increasing ER antagonism in Ishikawa cells. Analogues with cyclohexylaminoethoxy (**13a**) or adamantylaminoethoxy BSC (**13b**) lacking a polar aromatic ring displayed high ER-binding affinity and ER antagonism in Ishikawa cells higher than raloxifene and similar to fulvestrant (ICI182,780). The endometrial surface epithelium of immature female CD1 mice injected with **13b** was comparable to that of vehicle-treated mice, while that of mice treated with estradiol, raloxifene or **13b** in combination with estradiol was hyperplastic. These findings indicate that raloxifene analogues with a bulky BSC amino group could provide for higher endometrial safety treatment of the menopausal syndrome.

1. Introduction

Menopausal disorders can be treated with hormone therapy and more safely with selective ER modulators (SERMs) [1–3]. FDA-approved SERMs include among others, tamoxifen (for breast cancer prevention and treatment), raloxifene (for osteoporosis prevention and treatment and for invasive breast cancer prevention) and bazedoxifene in combination with equine estrogen (for prevention of osteoporosis and treatment of vasomotor symptoms) [2]. The health benefits of estrogen and SERMs are predominantly mediated by ER α and ER β 1, the estrogen-binding isoform of ER β . These are ligand-dependent transcription factors capable of regulating tissue and organ physiology by binding a large structurally diverse group of extraneous natural and synthetic chemicals besides estrogen [4,5]. ER α and ER β 1 modulate each other's transcriptional activity by acting as heterodimers as well as homodimers, with the heterodimers potentially targeting nearly half of the chromatin-binding sites that are accessible to the homodimers [6]. The pharmacology of SERMs is determined by the potential of SERM-bound ER to recruit functionally distinct co-regulators (co-activators and co-repressors) of

gene transcription in a cell-dependent manner, thus displaying different ER-agonist activities in different estrogen target cells [2,3]. Knockdown of Steroid Receptor Coactivator 1 expression by siRNA abolished ER-agonism of tamoxifen in uterine cells, suggesting that ER-agonism is dependent on the relative levels of expression of co-activators versus co-repressors [7]. ER-agonism in the uterus is the trait that predominantly determines the safety of SERMs [2,3]. Clinical studies have demonstrated that raloxifene maintains most of the breast cancer chemopreventive potential of tamoxifen and compared to the latter, it is associated with lower endometrial cancer risk [8]. On the whole, clinical studies support a safety profile for raloxifene [9]. Nevertheless, pre-clinical and clinical studies have shown that raloxifene can stimulate rat and human endometrium [10,11]. Bazedoxifene displayed lower uterotrophic activity compared to raloxifene and when tested in combination with conjugated estrogen (CE) failed to stimulate the endometrium [12]. In contrast, the combination of raloxifene with 17 β -estradiol (E2) or CE caused endometrial hypertrophy and hyperplasia [13].

ER-dependent recruitment of co-regulators to estrogen target gene enhancers is cell-, promoter- and ligand-specific [3]. Crystallographic

* Corresponding authors.

E-mail addresses: lambrinidis@pharm.uoa.gr (G. Lambrinidis), mikros@pharm.uoa.gr (E. Mikros), mnalexis@eie.gr (M.N. Alexis).

<https://doi.org/10.1016/j.bioorg.2020.104482>

Received 2 August 2020; Received in revised form 21 October 2020; Accepted 13 November 2020

Available online 17 November 2020

0045-2068/© 2020 Elsevier Inc. All rights reserved.

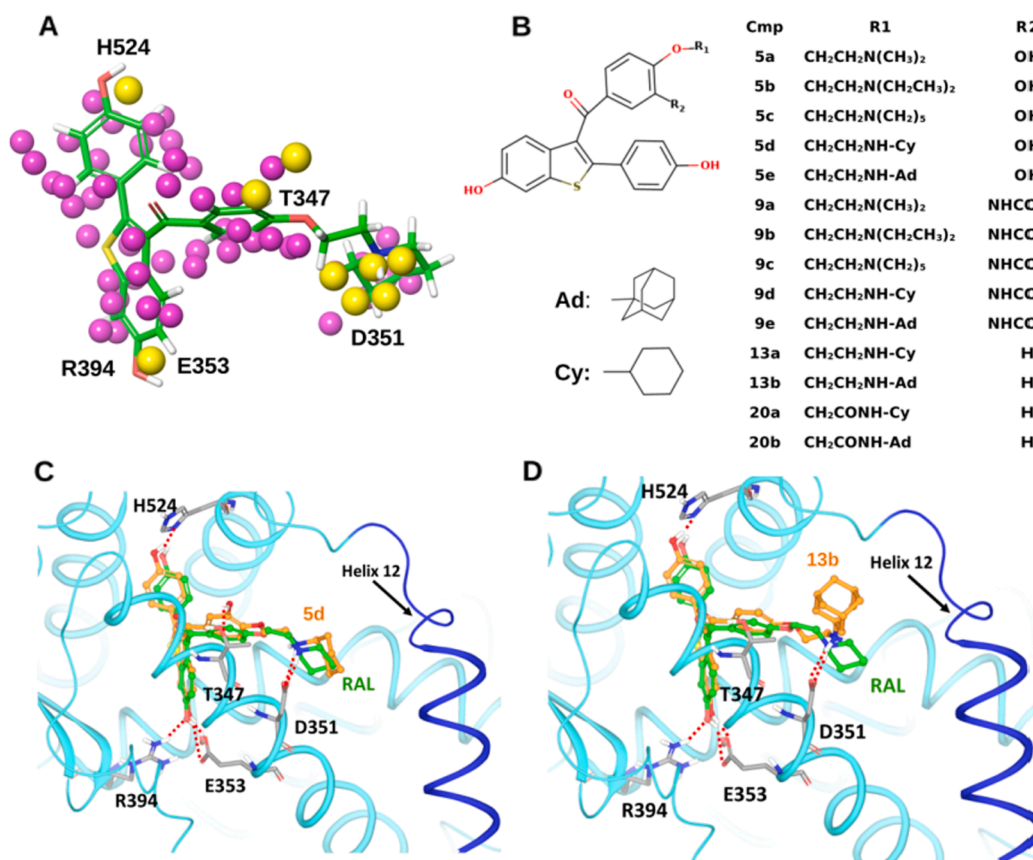


Fig. 1. (A) SZMAP analysis of ER α -LBD in complex with raloxifene. Hydrophobic and hydrophilic interfaces are colored purple and yellow, respectively. (B) Raloxifene analogues designed and synthesized based on SZMAP analysis. (C, D) Superimposition of the crystal structure of raloxifene (Ral) and the global minimum structure of **5d** (C) and **13b** (D) in complex with ER α -LBD; Ad: 1-adamantyl; Cy: cyclohexyl. (For interpretation of the references to colour in this figure legend, the reader is referred to the web version of this article.)

studies have shown that the agonist and antagonist activities of ER ligands are associated with distinct positions of the carboxyl-terminal alpha-helix 12 (H12) of the Ligand Binding Domain (LBD) of ER α and ER β [14–17]; binding of E2 to ER α allows H12 to form together with LBD H3 and H5 a binding site for co-activators, while binding of raloxifene allows its BSC to extend out of the ligand-binding pocket (LBP), interact with Asp351 and relocate H12 to the coactivator-docking site, thus stabilizing the antagonist conformation [14,17]. Likewise, positioning of H12 in-between the agonist and antagonist positions is associated with partial ER agonism, while failure of H12 to properly fold over the LBD exposes a sizeable hydrophobic domain, leading to proteasomal degradation of ER [15,16,18]. Recently, antiestrogens with an adamantyl core structure and BSC of varying length and/or bulkiness were reported, including two analogues with adamantylcarbonylamino or 3-hydroxypropylamido BSC end, of which the latter displayed ER α -antagonist efficacies comparable to fulvestrant (ICI182,780), a selective ER degrader (SERD) [19,20].

The aim of this study was to explore the impact of increasing bulkiness of the BSC amino group of raloxifene on ER agonism as well as the possibility to increase ER-binding affinity by introducing a fourth hydrogen bond. We initially synthesized two consecutive series of analogues with a BSC amino group of increasing bulkiness and a hydroxyl or an acetamide group at position 3' of the BSC aromatic ring for which preliminary Molecular Docking Simulations (MDS) predicted to form hydrogen bond with Thr347 of ER α or Thr299 of ER β . Since the analogues of both these series failed to display appreciable ER-binding affinity and/or low ER agonism, we next synthesized cyclohexylamino (**13a**) and adamantylamino (**13b**) BSC analogues lacking a 3'-derivatization and finally their respective amides for which preliminary MDS

predicted similar ER α -binding affinity to raloxifene. Compound **13a** has been patented by Eli Lilly but hasn't been biologically evaluated. The ER-binding affinity and inhibitory potency of the analogues and their efficacy of ER agonism and antagonism in breast and endometrial adenocarcinoma cells were assessed. We show that derivative **13b** is deprived of agonist activity in breast and endometrial cells and in the immature mouse uterus. These findings indicate that the adamantylamino BSC may help to develop SERMs of high endometrial safety.

2. Results and discussion

2.1. Rational design of modifications of the BSC of raloxifene

Crystal structures of raloxifene in complexes with the LBD of ER α and ER β (hereafter referred to as ER β) revealed that the BSC extends outwards from the center of the LBP through a predominantly hydrophobic channel to form a salt bridge between the piperidinium nitrogen and Asp351 of ER α (or Asp303 of ER β), thereby displacing H12 [15,16]. We followed the solvent mapping strategy in order to identify modifications that could increase chemical affinity. Using the SZMAP algorithm, as implemented on OpenEye Suite Software solvent mapping calculations, we identified significantly favorable or unfavorable regions of solvent thermodynamics in the LBP of ER α and ER β in the absence of ligand (apo form) as shown in (Fig. 1A). Water molecules interacting with the protein and stabilized through H bonds are shown with yellow spheres, while water molecules forcibly trapped within the protein are shown in purple. Superimposition of raloxifene shows that both core structure hydroxyl groups and BSC nitrogen coincide with yellow waters while all

Table 1
Predicted logP and experimental and theoretical $\Delta\Delta G$ of binding to ER α .

Test Cmp	RBA Exp ^a	LogP Pred	ΔG Exp ^b	$\Delta\Delta G$ Exp ^c	$\Delta\Delta G$ Pred ^d
Ral	62.9	6.48	-13.37	0.00	0.00
5a	7.01	4.69	-12.02	1.35	3.54
5b	13.68	5.35	-12.43	0.94	1.82
5c	6.51	5.43	-11.98	1.40	2.05
5d	23.45	4.59	-12.77	0.61	-0.12
5e	8.01	5.20	-12.10	1.27	1.05
9a	6.33	4.09	-11.96	1.42	4.79
9b	6.64	4.80	-11.99	1.39	2.89
9c	5.53	5.06	-11.88	1.50	4.89
9d	5.08	4.41	-11.82	1.55	3.85
9e	12.45	5.23	-12.38	1.00	0.90
13a	46.61	5.59	-13.19	0.18	-0.95
13b	20.51	6.39	-12.68	0.69	-2.34
20a	28.56	5.63	-12.89	0.49	nd
20b	13.51	5.60	-12.43	0.95	nd

^a Experimental relative binding affinity to ER α (RBA α) is expressed as % of that of estradiol (cf [Supplementary Table S1](#)).

^b Experimental ΔG (kcal/mol) of binding was calculated using Cheng Prusoff equation.

^c $\Delta\Delta G$ (kcal/mol): difference between the experimental ΔG of analogues from that of raloxifene.

^d $\Delta\Delta G$ (kcal/mol) of analogues from raloxifene as calculated using the FEP algorithm. Cmp: compound; Exp: experimental; Pred: predicted; Ral: raloxifene; nd: not determined

aromatic and hydrophobic surfaces overlap perfectly with purple waters. Drug design-wise however there is a specific yellow water molecule that does not match to a counterpart on raloxifene. This specific water molecule interacts with the hydroxyl group of Thr347 of ER α (Thr299 of ER β) located in the hydrophobic channel and oriented towards the aromatic ring of raloxifene BSC at a distance of 3.98 Å. This observation was utilized to design analogues initially with a hydroxyl group and subsequently with an acetamide group at position 3' of the BSC aromatic ring that potentially could form one or two H-bonds, respectively, with Thr347 (Thr299) and thus increase ER-binding affinity. The 3'-derivatized analogues were endowed with increasingly voluminous amino group substituents to examine whether increasing the basicity and bulkiness of the BSC amino group could perturb the conformational equilibrium of H12 and impact ER agonism by volume-induced

perturbations ([Fig. 1B](#), [5a-e](#) and [9a-e](#)). Since the experimental ER-binding affinity for these analogues was found to be considerably lower than that of raloxifene, though not as lower for those with a bulky BSC amino group as for the rest ([Table 1](#) and [Fig. 2](#)), we next synthesized cyclohexylamino and adamantylamino BSC analogues lacking 3'-derivatization ([13a](#), [13b](#)) and finally their amides ([20a](#), [20b](#)) to examine how the basicity and bulkiness of the BSC affect ER-binding affinity and ER agonism in the absence of interference from a 3'-derivatization. Notably, MDS indicated that the mode of binding of [13b](#) to ER α is driving the adamantylamino BSC to the outer space of the protein, which could stabilize H12 in the antagonist position and thus increase ER antagonist efficacy. [Fig. 2](#) conveys the rationales and the consequential experimental findings that guided the consecutive rounds of modifications of the BSC of raloxifene.

2.2. Theoretical molecular simulations

Preliminary docking simulations were run using the Induced Fit Docking (IFD) algorithm as implemented on Schrödinger Suite 2017. The first 10 analogues fitted well inside the binding pocket of ER, forming crucial hydrogen bonds. Like in raloxifene, the secondary amino groups of the BSC of [5d](#) ([Fig. 1C](#)) forms a salt bridge with Asp351, while a second inter-molecular hydrogen bond between the acidic phenolic hydroxyl group of its BSC and Thr347 stabilizes the conformation of the ligand. These 10 analogues were initially predicted to have similar binding affinity to raloxifene. The average variation of the free energy of binding (GlideScore) was relatively small, ~ 1.5 kcal/mol for ER α and ~ 2 kcal/mol for ER β , which is close to the standard error of prediction for molecular mechanic calculations. We then proceeded to more accurate Free Energy Perturbation (FEP) calculations for both raloxifene and analogue binding to ER α -LBD. These calculations could attribute differences in binding affinity to differences in solvation energy. For each pair of perturbations, we calculated the difference in the free energy of binding ($\Delta\Delta G$ Theoretical) ([Table 1](#)). As not expected, these analogues, with the exception of [5d](#), displayed lower ER-binding affinity compared to raloxifene. Nevertheless, we proceeded to their synthesis in order to evaluate how increasing the bulkiness of the BSC amino group would affect ER agonism. Then we carried out IFD simulations for the two bulky BSC analogues lacking a 3'-derivatization ([13a](#), [13b](#)) and their respective amides ([20a](#), [20b](#)) and FEP calculations for the former

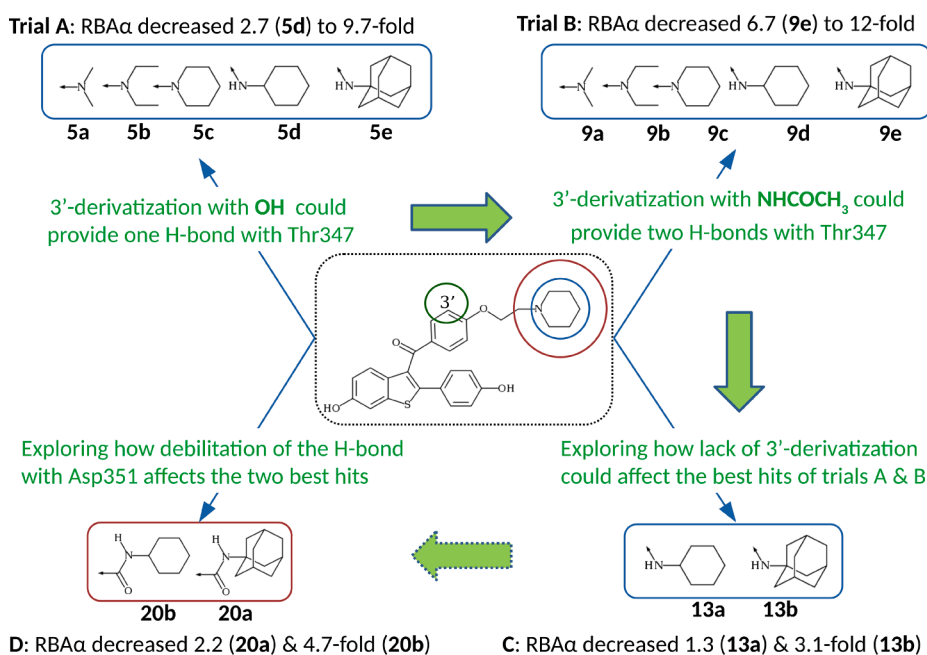
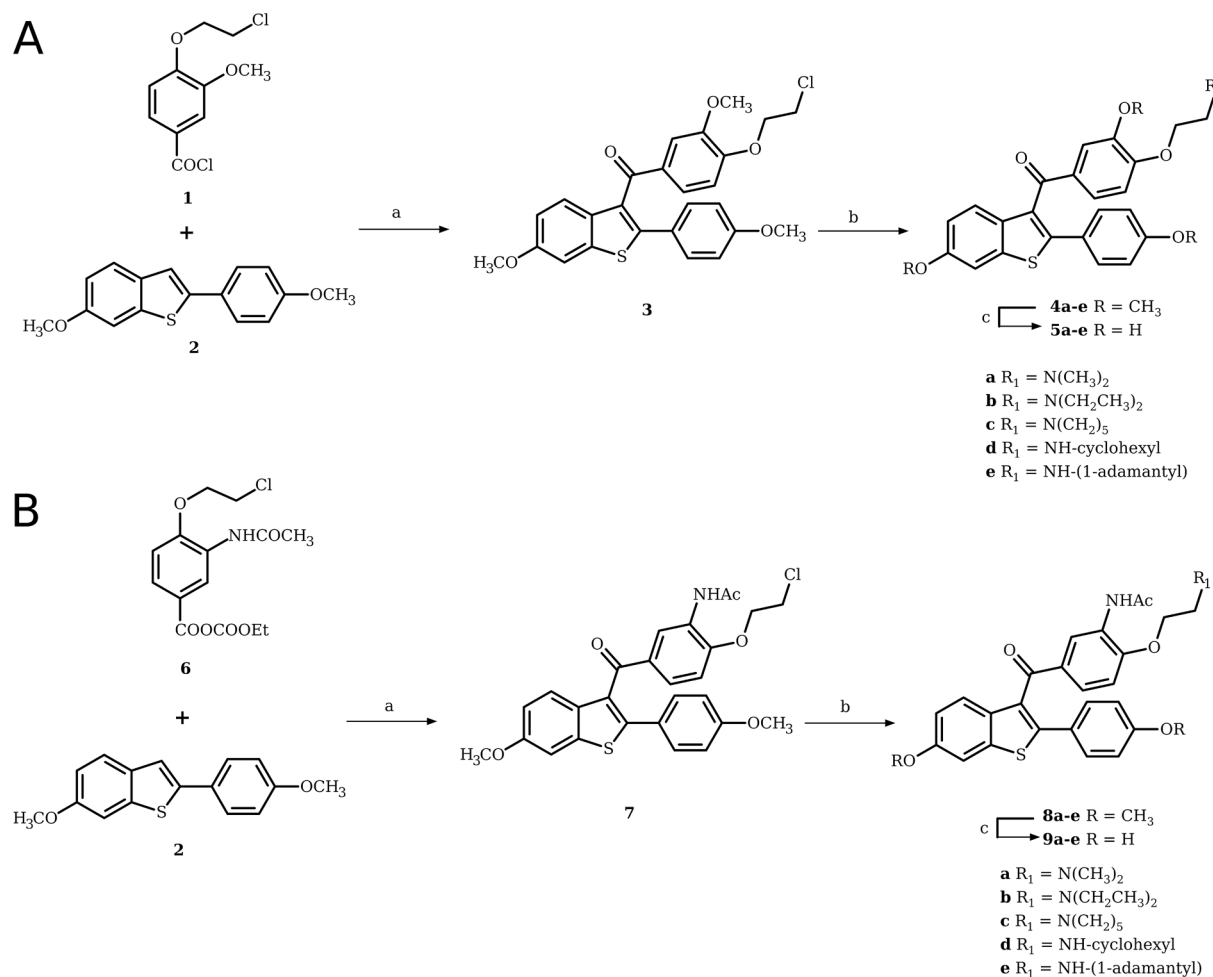


Fig. 2. Design and synthesis of basic side chain (BSC) analogues of raloxifene: Introduction of a hydroxyl and subsequently of an acetamide group at position 3' of the BSC aromatic ring and of increasingly voluminous amino group substituents to the 3'-derivatives gave rise to analogues of appreciably lower RBA α compared to raloxifene. Since RBA α decrease was comparatively lower for analogues with bulkier BSC amino groups ([5d](#), [9e](#)), cyclohexylamino and adamantylamino BSC analogues lacking 3'-derivatization ([13a](#), [13b](#)) were synthesized next followed by their amides ([20a](#), [20b](#)) in order to examine how the basicity and bulkiness of the BSC amino group affected RBA α in the absence of 3'-derivatization.



Scheme 1. (A), a) 6-methoxy-2-(4-methoxyphenyl)benzoyl chloride (**1**), AlCl₃, 1,2 DCE, rt, 1 h; b) Amine, EtOH, reflux, 24 h; c) AlCl₃, EtSH, CH₂Cl₂, rt, 2 h. (B), a) **2**, AlCl₃, 1,2 DCE, rt, 1 h; b) Amine, EtOH, rt, 24 h; c) AlCl₃, EtSH, CH₂Cl₂, rt, 2 h.

(Fig. 1D). While IFD simulations predicted for **13a** and **13b** affinities comparable to or lower than that of raloxifene, FEP calculations predicted affinities higher than raloxifene (Table 1). In the light of these findings, we proceeded to the synthesis of all 4 analogues lacking a 3'-derivatization.

2.3. Synthesis

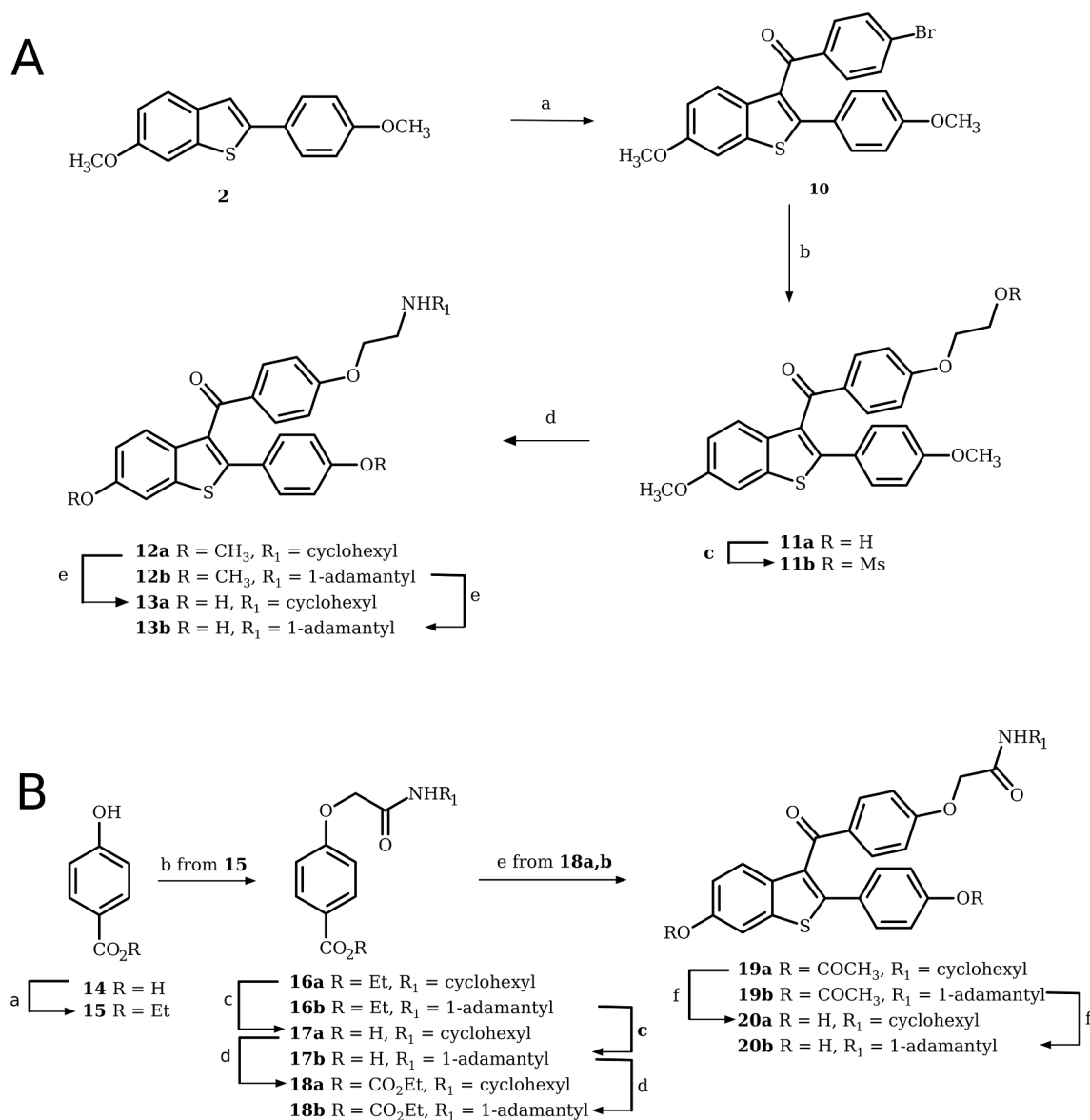
Derivatives **4a-e** (Scheme 1A) were prepared from the benzoyl chloride **1**, which was easily obtained from the corresponding carboxylic acid [21,22]. The chloride **1** was then used for the acylation of 6-methoxy-2-(4-methoxyphenyl)benzo[b]thiophene (**2**) [23] and the resulting benzothiophene **3** was treated with the appropriate primary or secondary amines to give compounds **4a-e**, which upon deprotection yielded the target compounds **5a-e**. Analogues **9a-e** (Scheme 1B) were prepared from the mixed anhydride **6** by an analogous procedure. Compound **6** was prepared from ethyl 3-amino-4-hydroxybenzoate [24] by successive *N*-acetylation, etherification, ester hydrolysis and treatment of the substituted benzoic acid with ethyl chloroformate (for compound synthesis, isolation and characterization see Supplementary Material).

The secondary amines **13a,b** (Scheme 2A) were prepared by the procedure proposed by Bradley et al [25] using the benzothiophene **2** [23] as starting material. Compound **2** was acylated with 4-bromobenzoylchloride and the bromine atom of the resulting ketone **10** [26,27] was displaced by 2-hydroxyethoxide to give compound **11a** [25,27], which was converted to the corresponding mesylate **11b**. Treatment of

the mesylate with the suitable amines resulted in the benzothiophenes **12a,b** which upon demethylation produced the target amines **13a** and **13b** [27]. Finally, the amides **20a,b** (Scheme 2B) were prepared from ethyl 4-hydroxybenzoic acid (**15**) which reacted with *N*-cyclohexyl- or *N*-(1-adamantyl)-2-chloroacetamide to give the carboxamides **16a** and **16b**, respectively [both compounds were synthesized, although they could be purchased from chemical vendors]. The carboxamides were then converted first to the corresponding carboxylic acids **17a,b** and then to the mixed anhydrides **18a,b**, which were used for the Friedel-Crafts acylation of 6-acetyloxy-2-(4-acetyloxyphenyl)benzo[b]thiophene [23] that provided the benzo-thiophenes **19a,b**. These were deprotected to give the target compounds **20a,b**.

2.4. ER α - and ER β -binding affinities

The affinity and selectivity of analogue binding to ER α and ER β were assessed relative to the binding affinity (set to 100) and selectivity (set to 1) of E2 using competitor assay kits, as already described [28]. The relative binding affinities of the analogues for ER α (RBA α) were from 1.3-fold (**13a**) to 12.3-fold (**9d**) lower compared to raloxifene, while for ER β (RBA β) were from 1.6-fold (**13a**) to 42-fold (**9b**) lower; as well, the RBA α :RBA β ratio of the analogues ranged between 1.2 (**13b**) and 7.3 (**9b**), while that of raloxifene was 1.7, suggesting very low to average selectivity of the analogues for ER α . Interestingly, **13b** displayed a RBA α :RBA β of 1.2, indicating that the adamantylamino group can be accommodated nearly equally well in the LBD of ER α and ER β (for RBA values and ratios see Supplementary Table S1, columns 2–4). The



Scheme 2. (A), a) EtOH, HCl (gas), reflux, 2 h; b) K_2CO_3 , acetone, $ClCH_2CONHR_1$, reflux, 12 h; c) NaOH 40%, EtOH, rt, 1 h; d) toluene, $ClCO_2Et$, Et_3N , 0 °C, 1 h; e) 6-acetyloxy-2-(4-acetyloxyphenyl)benzo[b]thiophene, $AlCl_3$, 1,2-DCE, rt, 1 h; f) MeOH/ NH_3 , rt, 1 h. (B), a) 4-bromobenzoylchloride, $AlCl_3$, 1,2 DCE, rt, 1 h; b) NaH, $HOCH_2CH_2OH$, DMF 90 °C, 1 h; c) MsCl Et_3N , CH_2Cl_2 , rt, 1 h; d) cyclohexylamine or 1-adamantanamine, KI, toluene, reflux, 12 h; e) $AlCl_3$, EtSH, CH_2Cl_2 , rt, 2 h.

introduction of a hydroxyl or an acetamide group at position 3' of the BSC phenyl group was expected to increase RBA as already explained in Section 2.1. However, derivatization of raloxifene at position 3' to generate **5c** and **9c** decreased RBA_α 9.7- and 11.4-fold, respectively, and RBA_β 10.8 and 25.3-fold, respectively, indicating that these derivatizations are incompatible with BSC channel constrains of either ER. In fact, the RBA_α and RBA_β of the 3' derivatives were 4.6- to 12.3-fold and 5.8- to 42.1-fold lower, respectively, than those of raloxifene, implying that, irrespective of the volume of the amino group substituent, derivatization at position 3' is more incompatible with the hydrophobicity constrains of the BSC channel of ER β than with those of ER α . The role of hydrophobicity in inducing affinity variations among the analogues **5a-e** and **9a-e** is discussed in the below subsection. Given that tertiary amines are less basic than secondary ones, it was not expected that replacement of a tertiary BSC amino group (raloxifene) by a more basic secondary one (**13a**, **13b**) (a replacement that would increase the pK_a value from 8.46 to 10.07, as calculated from Marvin Sketch software), would lower RBA_α and RBA_β . It appears that the lower RBA of **13a** and **13b** compared to raloxifene may reflect steric hindrance owing

to the increased length and/or bulkiness of the BSC and/or entropy-enthalpy compensation as discussed in the following subsection. Delocalization of the lone electron pair of amide nitrogen likely accounts for the lower RBA_α and RBA_β of **20a** and **20b** compared to **13a** and **13b**. Notably, stabilization by a salt bridge is known to be considerably stronger than stabilization by weakly charged partners. Finally, the approx. 2.2-fold lower RBA_α of **20b** compared to **20a** and of **13b** compared to **13a** could reflect the increased bulkiness of the adamantylamino group compared to the cyclohexylamino one.

The preliminary FEP calculations of $\Delta\Delta G$ evidently overestimated the binding affinity of the cyclohexylamino and adamantylamino analogues (Table 1). We therefore explored other factors influencing the binding interactions. Calculated $\log P$ values (Marvin Sketch 19.20) were in very good correlation with $\Delta G_{\text{binding}}$ (Fig. 3A), depicting the importance of hydrophobic interactions and the entropic term of the free energy of these interactions for the ER-binding affinity. Using Ligand and Structure-Based Descriptors analysis (LSBD, Schrödinger Inc), 180 descriptors were calculated and partial least squares (PLS) analysis resulted to an improved correlation between experimental and calculated

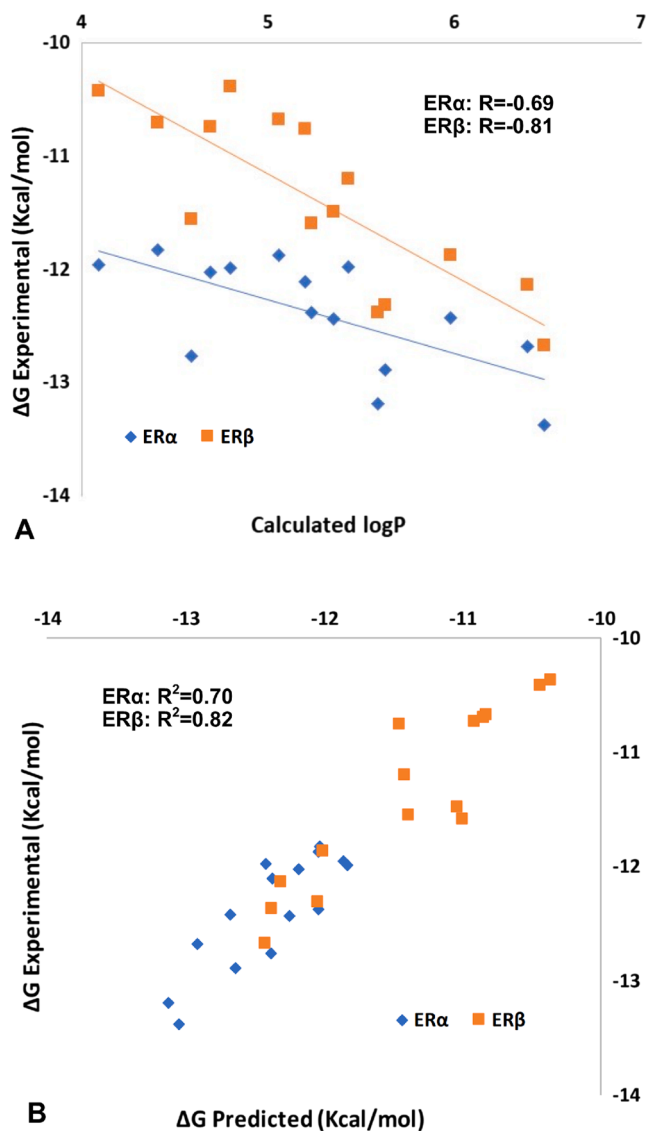


Fig. 3. Correlation between the experimental ΔG of binding of raloxifene and its analogues to ER α and ER β and, A) calculated logP and, B) ΔG of binding as calculated using LSBD analysis.

data (Fig. 3B). LSBD analysis takes into account topological and lipophilicity descriptors of each ligand, as well as interaction energy terms from all different algorithms (Glide, Liaison, Embrace, etc), combining them to a final prediction model. The descriptors influencing most the final model were associated with lipophilicity and solute-accessible surface area.

Since secondary amines are less lipophilic than tertiary ones ($\log P_{13a} = 5.59$ while $\log P_{RAL} = 6.48$), it is possible that the logP value of raloxifene is a crucial cutoff favoring binding vs solubility. Although docking calculations predicted that an OH or a NHCOCH₃ group at the 3'-position of BSC phenyl group could improve affinity, all the 3'-derivatives displayed lower RBA than raloxifene. A rationalization based on the decrease of lipophilicity of all the 3'-derivatives compared to raloxifene would be most suitable, given the trends observed in Fig. 3A. It is clear, however, that binding to ER is a multivariate process and that several factors (partial charge of BSC nitrogen, logP, pKa) affect the binding affinity. In the FEP calculations we obtained a very good overall correlation ($r = 0.8$) between predicted and experimental $\Delta\Delta G$ (Fig. 3B). However, while FEP calculations showed that **13a**, **13b** and possibly **5d** should have displayed better binding affinity compared to raloxifene (Table 1, column 6), for most of the remainder analogues the solvation

energy of perturbation was predicted to be lower compared to the experimental one. ER β FEP calculations predicted even better binding optimization (data not shown). Overall, however, the introduction of a polar group on raloxifene BSC in order to improve the enthalpy of interaction through formation of H bond(s) with Thr347 (Thr299) appears to be detrimental for affinity, probably because is counterbalanced by unfavorable entropic contributions commonly referred to as enthalpy-entropy compensation [29].

2.5. Potency of antagonism of ER-mediated effects

We investigated whether and how RBA correlated with the potency of antagonism of E2-induced ER-dependent, (i) gene transcription in MCF7:D5L cells (a clone of MCF7 cells stably transfected with an ERE-endowed luciferase reporter gene [30]), (ii) proliferation of wild-type MCF7 cells and, (iii) alkaline phosphatase (AlkP) expression in Ishikawa cells; while (i) and (ii) depend on ER α , (iii) depends on both ER α and ER β [31]. The potency of antagonism (IC₅₀) was assessed using cells growing in medium supplemented with charcoal-treated heat-inactivated (i.e. steroid-free) fetal bovine serum (chFBS) and 0.1 nM E2 i.e. post-menopausal level of estrogen. The E2-repleted cells were exposed to vehicle (0.1% DMSO) or to increasing concentrations of test compounds for 24 h (MCF7:D5L cells) or 72 h (MCF7 and Ishikawa cells) (Figs. 4A,B,C and 5A,C). Only 2 analogues (**13a**,**13b**) displayed IC₅₀ of antagonism of E2-induced transcription lower than 20 nM (Table 2, column 4); their IC₅₀ of antagonism of E2-induced MCF7 cell proliferation were 1.51 nM (**13a**) and 5.80 nM (**13b**) and of E2-induced AlkP expression 10.6 nM (**13a**) and 8.27 nM (**13b**) (for IC₅₀ comparisons see Supplementary Table S1, columns 5–7). The structure-activity relationships (SARs) of the analogues based on the IC₅₀ of ER-dependent gene transcription and those of cell proliferation correlated with RBA α [Pearson's $R = -0.419$ ($p = 0.021$) and -0.791 ($p = 0.001$), respectively], as expected from cells (MCF7:D5L and MCF7) known to express only ER α , while the IC₅₀ of AlkP expression correlated with RBA β ($R = -0.547$; $p = 0.043$), in line with the involvement of ER β in the E2-dependent expression of AlkP [31].

2.6. Efficacy of agonism and antagonism of ER-mediated effects:

The agonist and antagonist efficacies of analogues compared to raloxifene were assessed using cells growing in chFBS supplemented with vehicle (agonist mode) or 0.1 nM E2 (antagonist mode); the full antagonist ICI182,780 (ICI) was used as control. In the antagonist mode (Figs. 4A,B,C and 5A,C), with the ER-antagonist efficacy of ICI (1 μ M) and E2 (0.1 nM) set equal to 100% and 0%, respectively, **13a** and **13b** displayed lower antagonist efficacy compared to ICI in MCF7:D5L cells and similar antagonist efficacy to ICI in MCF7 cells, while raloxifene displayed similar antagonist efficacy to ICI in either cell. In Ishikawa cells, however, the antagonist efficacy of **13b** was higher compared to ICI, while that of **13a** was comparable to ICI and that of raloxifene and all the other analogues was lower compared to ICI (for antagonist efficacy comparisons see Supplementary Table S2, columns 2–4). Notably, the rank order of antagonist efficacies of the key analogues in Ishikawa cells was, **13b** > ICI \approx **13a** > raloxifene ($p < 0.05$; ANOVA), indicating that ER antagonism increased as the bulkiness of the BSC amino group increased.

The higher antagonist efficacy of **13b** compared to **13a** in Ishikawa cells may reflect a higher potential of **13b** to favor formation of ER α /ER β heterodimers over homodimers, resulting in improved corepressor recruitment through ER β . It is anticipated that formation of ER α /ER β heterodimers is favored when RBA α and RBA β are comparable, which is the case with **13b** more than with any other analogue. It has been reported that in ER α /ER β -expressing cells the coregulator RIP140 can undertake corepressor functions upon recruitment by ER β [6]. Interestingly, using glutamate-challenged HT22 cells to assess the

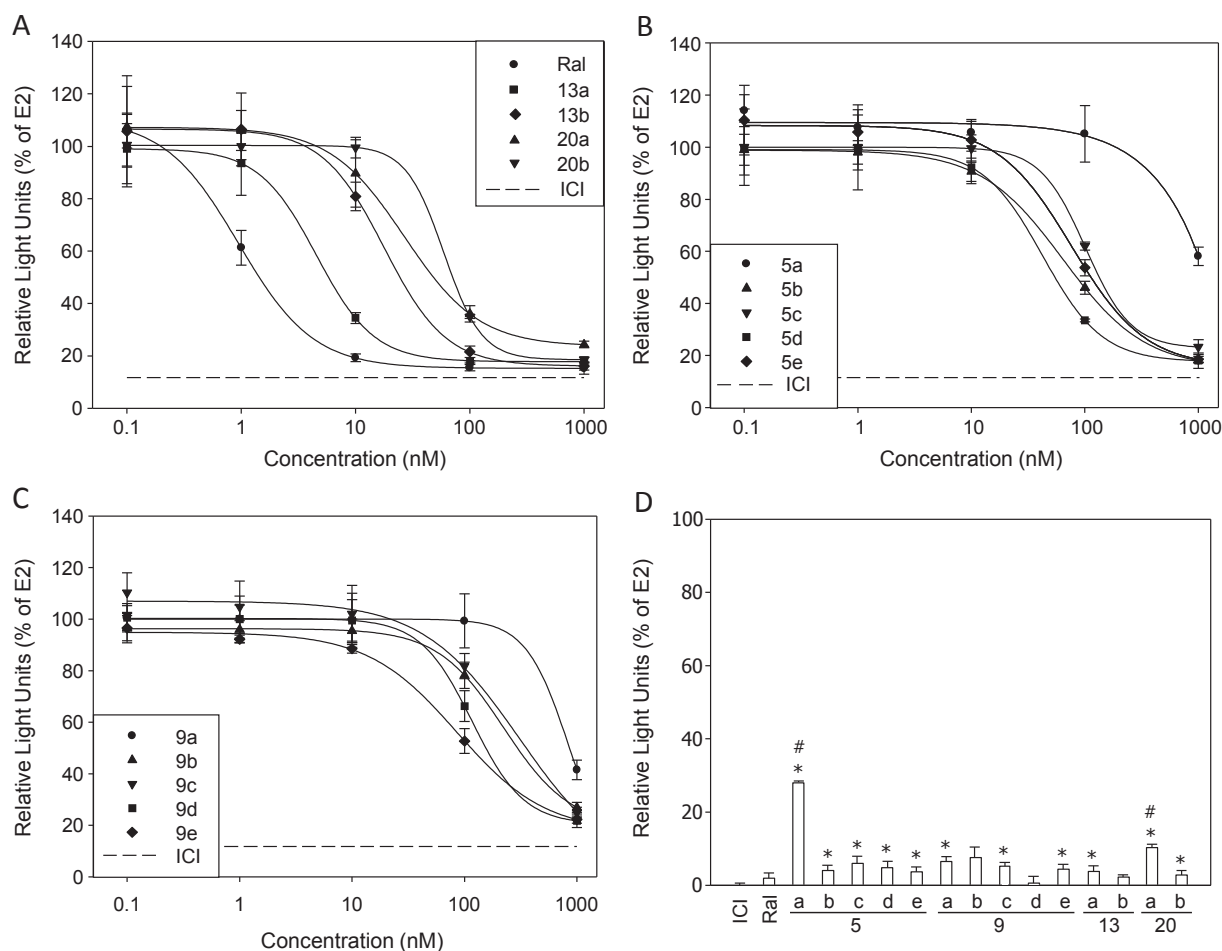


Fig. 4. Estrogen receptor agonism and antagonism of raloxifene and its analogues in ERE-dependent gene transcription. MCF7:D5L cells growing in culture medium supplemented with 5% chFBS and either 0.1 nM estradiol (E2) (antagonist mode, A-C) or vehicle (agonist mode, D), were treated for 16 h with increasing concentrations of raloxifene (Ral) or Ral analogue or 1 μ M ICI182,780 (ICI) (A-C); or with 1 μ M Ral or Ral analogue or ICI or 0.1 nM E2 (D). Luciferase expression was expressed relative to that in the presence of 0.1 nM E2, set equal to 100. Data are mean \pm SEM of at least three independent experiments carried out in triplicate. *, # $p < 0.05$ vs incubation with ICI or raloxifene, respectively (ANOVA); shFBS, charcoal-treated heat-inactivated fetal bovine serum.

antioxidant activity of **13b** vs that of raloxifene, as previously reported [32], revealed that **13b** was moderately active while raloxifene was inactive in this assay (Supplementary Fig. S1), presumably reflecting adamantane's electron donor potential due to its hyperconjugation properties [33]. Whether this potential is somehow involved in stabilizing the antagonist conformation of ER α and/or ER β is unknown.

In the agonist mode (Figs. 4D and 5B,D), with the agonist efficacy of E2 (0.1 nM) and ICI (1 μ M) set equal to 100% and 0%, respectively, **13a** displayed higher agonist efficacy than ICI in MCF7:D5L cells and similar agonist efficacy to ICI in MCF7 cells, while **13b** and raloxifene displayed similar agonist efficacy to ICI in both cells. In Ishikawa cells, however, the agonist efficacy of **13b** was lower compared to ICI, while that of **13a** was comparable to ICI and that of raloxifene and all the other analogues was higher compared to ICI (Supplementary Table S2, columns 5–7). Notably again, the rank order of agonist efficacies of the key analogues at 1 μ M in Ishikawa cells was, raloxifene > ICI \approx **13a** > **13b**, implying that ER agonism decreased as the bulkiness of the BSC amino group increased. In line with this notion, the rank order of relative agonist efficacies in the **5a:b:c:d:e** series was 1.0:0.8:0.8:0.4:0.1 and in the **9a:b:c:d:e** series 1.0:0.9:0.8:0.7:0.6. Again, these data argue in favor of a suppressive effect of bulkiness on ER agonism in Ishikawa cells. The SARs of the analogues as ER agonists are summarized in Table 2. The inference from the SARs data of Table 2 is that finding a means (e.g. a core structure modification) for increasing the antagonist potency (IC₅₀) of **13b** (lowest agonist efficacy hit) might generate SERMs of therapeutic

potential as well as endometrial safety.

The ability of **13a** and **13b** to antagonize MCF7 cell proliferation as effectively as raloxifene and AlkP expression in Ishikawa cells more effectively than raloxifene prompted a comparison of their effects on the proliferation of these cells in the presence of FBS and chFBS. In the presence of FBS and 0.1 nM E2, raloxifene, **13a**, **13b** and ICI (all at 1 μ M) suppressed MCF7 cell proliferation fully and Ishikawa cell proliferation marginally (raloxifene) or partially (**13a**, **13b** and ICI) (Supplementary Fig. S2A,B). Interestingly, in Ishikawa cells, the partial suppressive effects of **13a** and **13b** were similar to the effect of ICI. Likewise, in the presence of chFBS and 0.1 nM E2, raloxifene, **13a**, **13b** and ICI (all at 1 μ M) suppressed MCF7 and Ishikawa cell proliferation fully and partially, respectively (Supplementary Fig. S2C,D). Again, in Ishikawa cells, the suppressive effects of **13a** and **13b** were similar to the effect of ICI. Since the ER α of MCF7 cells was degraded in the presence of ICI but not in the presence of raloxifene, **13a** or **13b** (inset to Supplementary Fig. S2C and data not shown), the mechanism of action of raloxifene and its analogues is likely different from that of ICI. These findings classify **13a** and **13b** as SERMs rather than SERDs. Given the many adverse effects of ICI, including detrimental effect on bone mineral density and femoral strength [3], it is tempting to speculate that **13a** and **13b** might be devoid of such effects. Recently, antiestrogens with an adamantyl ligand core structure and an adamantylcarbonylamino group in the BSC end facing H11 and H12 were shown to display considerable ER α -antagonist and ER α -degrading activities, albeit lower compared to those of ICI [20].

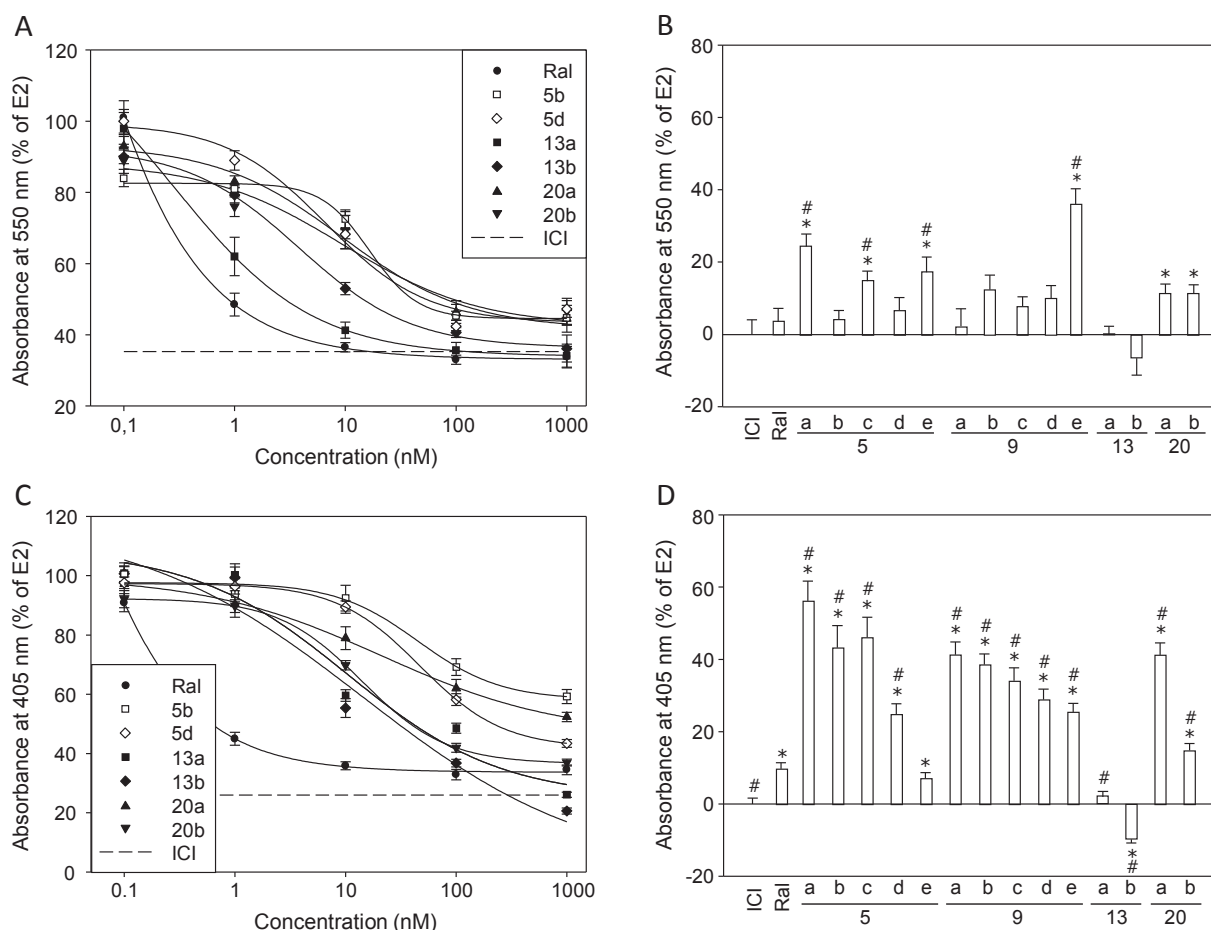


Fig. 5. Estrogen receptor agonism and antagonism of raloxifene and its analogues in cell proliferation and alkaline phosphatase expression. MCF7 cells (A, B) and Ishikawa cells (C, D) growing in culture medium supplemented with 5% chFBS plus either 0.1 nM estradiol (E2) (antagonist mode, A, C) or vehicle (agonist mode, B, D) were treated for 72 h with increasing concentrations of raloxifene (Ral) or Ral analogue or with 1 μ M ICI182,780 (ICI) (A, C); or with 0.1 nM E2, or 1 μ M of Ral or Ral analogue or ICI (B, D). Relative cell numbers were assessed using MTT (A, B), AlkP expression was assessed by measuring pNPP hydrolysis at 405 nm (C, D), and both were expressed relative to the respective values in the presence of 0.1 nM E2 set equal to 100. Data are mean \pm SEM of at least three independent experiments carried out in triplicate. *, # $p < 0.05$ vs incubation with ICI or raloxifene, respectively (ANOVA); pNPP, *para*-Nitrophenylphosphate; shFBS, charcoal-treated heat-inactivated fetal bovine serum.

2.7. Effects on the immature mouse uterus

Analogue **13b** was singled out for in vivo assessment. Immature female CD1 mice weighing 13.1 ± 0.5 g received daily for three consecutive days subcutaneous injections of vehicle (20 μ l of DMSO), E2 (55 μ g/kg), raloxifene (9.5 mg/kg), **13b** (10 mg/kg) or **13b** followed 1 h later by E2 (55 μ g/kg) before subjecting them to euthanasia on the fourth day. Histological examination of hematoxylin/eosin-stained uterine sections revealed that in the vehicle-treated group of animals, the surface endometrium had a mean height of 51.76 μ m. The architecture and distribution of glands in the stroma appeared to be normal, without features of hyperplasia. Rare mitotic figures were recognized in the surface and glandular endometrial epithelium (1 Mitotic Figure/10 High Power Fields) (Fig. 6A). The endometrial surface epithelium of E2-treated mice was prominently hyperplastic compared to that of vehicle-treated animals, with a mean height of 69.55 μ m. Hyperplasia of the glandular epithelium and endometrial glands (proliferation of glands, with an increase in the gland to stroma ratio compared to normal endometrium, and back-to-back glands) was also observed. Furthermore, there was an increase in the number of apoptotic bodies in the glandular epithelium and in the mitotic activity of the stroma (7–8 MF/10 HPF) compared to vehicle-treated mice (Fig. 6B). In the group of raloxifene-treated animals, prominent hyperplasia of the surface endometrium was observed, with a mean height of 61.24 μ m. Mitotic figures

were numerous in the surface epithelium (7 MF/10 HPF). The endometrial glands were hyperplastic with fewer apoptotic bodies compared to the E2 group. The endometrial stroma appeared to be edematous (Fig. 6C). The mean height of surface epithelium of **13b**-treated animals was 55.08 μ m, showing extremely mild hyperplasia compared to vehicle-treated mice. Hyperplasia of endometrial glands was present. Mitotic activity was increased in the surface and in the glandular epithelium compared to vehicle-treated animals, though not as excessively as in the raloxifene-treated ones (4 MF/10 HPF) (Fig. 6D). In the group of animals treated with **13b** followed by E2, the surface endometrium appeared highly hyperplastic with a mean height of 71.63 μ m. Hyperplasia and increased mitotic activity (5 MF/10 HPF) were observed in the endometrial glands compared to vehicle-treated mice. The endometrial stroma appeared mildly edematous in some areas, with a slight increase in mitotic figures (2 MF/10 HPF) compared to vehicle-treated mice though not so pronounced as in E2-treated animals (Fig. 6E). Analysis of microscope images using ImageJ (<http://imagej.net>) revealed that, compared to the surface epithelium of vehicle-treated mice, that of the other animals was significantly thicker, with the exception of the surface epithelium of **13b**-treated ones (Fig. 6F).

It has been reported that raloxifene exerts a trophic effect in the immature rodent uterus [10,12]. The above findings confirm these reports and further show that while raloxifene caused prominent hyperplasia of surface endometrium and endometrial glands, **13b** was only

Table 2
SARs of raloxifene analogues.

	R1	R2	IC ₅₀ ^a (nM)	Agonism ^b (% of E2)
5a	CH ₂ CH ₂ N(CH ₃) ₂	OH	~1000	56.4
5b	CH ₂ CH ₂ N(CH ₂ CH ₃) ₂	OH	61.5	43.5
5c	CH ₂ CH ₂ N(CH ₂) ₅	OH	109	46.4
5d	CH ₂ CH ₂ NH-Cy	OH	40.9	25.1
5e	CH ₂ CH ₂ NH-Ad	OH	86.9	7.4
9a	CH ₂ CH ₂ N(CH ₃) ₂	NHCOCH ₃	734	41.6
9b	CH ₂ CH ₂ N(CH ₂ CH ₃) ₂	NHCOCH ₃	222	38.9
9c	CH ₂ CH ₂ N(CH ₂) ₅	NHCOCH ₃	263	34.3
9d	CH ₂ CH ₂ NH-Cy	NHCOCH ₃	124	29.2
9e	CH ₂ CH ₂ NH-Ad	NHCOCH ₃	77.7	25.7
13a	CH ₂ CH ₂ NH-Cy	H	4.59	1.1
13b	CH ₂ CH ₂ NH-Ad	H	19.4	-9.8
20a	CH ₂ CONH-Cy	H	35.2	41.5
20b	CH ₂ CONH-Ad	H	60.4	15.1
Ral	CH ₂ CH ₂ N(CH ₂) ₅	H	1.11	10.0

^a Potency of antagonism of ER-dependent gene transcription in MCF7:D5L cells.

^b Efficacy of agonism of AlkP expression in Ishikawa cells; Cmp: compound; E2: estradiol; Ad: 1-adamantyl; Cy: cyclohexyl.

group of the BSC of raloxifene in order to H-bond Thr347 (ER α) or Thr299 (ER β) as well as increasing the bulkiness of its BSC amino group would generate analogues of similar ER-binding affinity to raloxifene. Since the ER-binding affinity of the 3'-derivatives was found to be considerably lower than that of raloxifene, the inference is that the 3'-derivatizations clash with the BSC channel constraints. The two analogues lacking a 3'-derivatization and bearing cyclohexylamino (**13a**) and adamantylamino BSC (**13b**) subsequently synthesized, displayed high affinity for ER α and ER β and antagonist efficacy in Ishikawa cells higher than raloxifene and similar to (**13a**) or higher than (**13b**) ICI. Unlike the latter, however, these two analogues preserved ER α integrity, implying that they could be classified as SERMs rather than SERDs. Importantly, while the endometrial surface epithelium of immature female mice injected with **13b** was comparable to that of vehicle-treated mice, the surface epithelium of mice treated with **13b** in combination with estradiol was highly hyperplastic. The above findings suggest that inventing a means for increasing the ER-binding affinity and consequently the antagonist potency of the adamantylaminoethoxy analogue may give rise to SERMs of higher endometrial safety for the treatment of menopausal syndrome.

4. Experimental Section

The Experimental Section is presented in the [Supplementary Material](#).

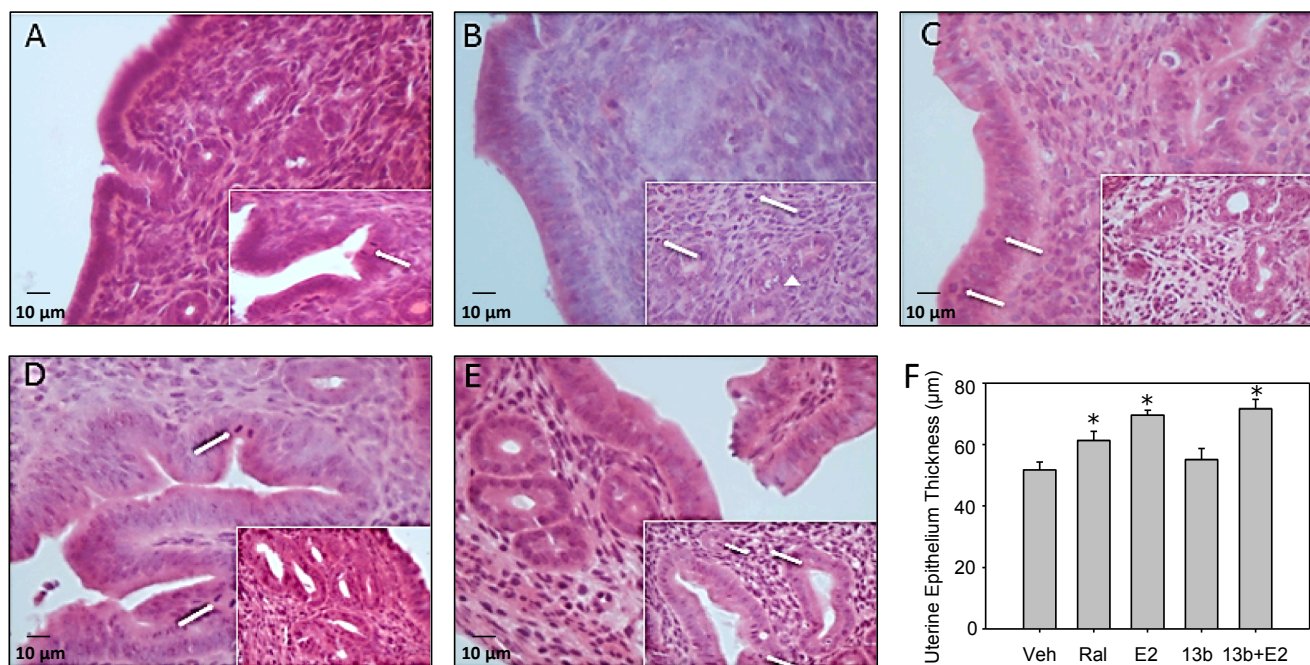


Fig. 6. A (vehicle): Normal endometrium. Glands with normal architecture and distribution [inset: mitosis in surface endometrium (arrow)]; B (estradiol): Hyperplasia of surface endometrial epithelium [inset: Increased stromal mitotic activity (arrows) and crowded endometrial glands with apoptotic bodies (arrowhead)]; C (raloxifene): Hyperplasia and increased mitotic activity in surface endometrial epithelium (arrows) [inset: edematous stroma and glandular hyperplasia]; D (**13b**): Mild hyperplasia and mitotic activity in surface endometrial epithelium (arrows) [inset: Endometrial glandular hyperplasia]; E (**13b** + estradiol): Hyperplasia of surface endometrial epithelium and endometrial glands, and edematous stroma [inset: Increased mitotic activity in glands and stroma (arrows)]; F: Average luminal epithelial height: values are mean \pm SEM of ten independent assessments (* $p < 0.05$ compared to vehicle; t -test. A-E, mag x400).

mildly active in either respect; and that **13b** was able to suppress hormonal induction of mitotic activity in the stroma but not in the surface endometrium and endometrial glands.

3. Conclusion

Preliminary molecular mechanic calculations suggested that introducing a hydroxyl or an acetamido group at position 3' of the phenyl

Declaration of Competing Interest

None of the authors has a conflict of interest to declare.

Acknowledgments

We thank Nikos Youroukos, Animal Facility Unit, National Hellenic Research Foundation, for his assistance with animal experiments. This

study was carried out with the financial support of Thales 2011 program “SERMENCO MIS 375617”, which was co-funded by the European Social Fund and National Resources.

Appendix A. Supplementary material

Supplementary Material includes Tables S1-2; Fig. S1-2; Theoretical Molecular Methods; Chemical Synthesis Methods; Biological Evaluation Methods; ^1H and ^{13}C spectra of synthesized compounds; References. Supplementary data to this article can be found online at <https://doi.org/10.1016/j.bioorg.2020.104482>.

References

- [1] J. Marjoribanks, C. Farquhar, H. Roberts, A. Lethaby, J. Lee, Long-term hormone therapy for perimenopausal and postmenopausal women, *Cochrane Database Syst. Rev.* (2017), <https://doi.org/10.1002/14651858.CD004143.pub5>.
- [2] J.V. Pinkerton, S. Thomas, Use of SERMs for treatment in postmenopausal women, *J. Steroid Biochem. Mol. Biol.* 142 (2014) 142–154, <https://doi.org/10.1016/j.jsmb.2013.12.011>.
- [3] S.E. Wardell, E.R. Nelson, D.P. McDonnell, From empirical to mechanism-based discovery of clinically useful Selective Estrogen Receptor Modulators (SERMs), *Steroids* 90 (2014) 30–38, <https://doi.org/10.1016/j.steroids.2014.07.013>.
- [4] G.G.J.M. Kuiper, J.G. Lemmen, B. Carlsson, J.C. Corton, S.H. Safe, P.T. van der Saag, B. van der Burg, J.-Å. Gustafsson, Interaction of estrogenic chemicals and phytoestrogens with estrogen receptor β , *Endocrinology* 139 (1998) 4252–4263, <https://doi.org/10.1210/endo.139.10.6216>.
- [5] G. Lambrinidis, M. Halabalaki, E.S. Katsanou, A.-L. Skaltsounis, M.N. Alexis, E. Mikros, The estrogen receptor and polyphenols: molecular simulation studies of their interactions, a review, *Environ. Chem. Lett.* 4 (2006) 159–174, <https://doi.org/10.1007/s10311-006-0065-y>.
- [6] Z. Madak-Erdogan, T. Charn, Y. Jiang, E.T. Liu, J.A. Katzenellenbogen, B. S. Katzenellenbogen, Integrative genomics of gene and metabolic regulation by estrogen receptors α and β , and their coregulators, *Mol. Syst. Biol.* 9 (2013) 676, <https://doi.org/10.1038/msb.2013.28>.
- [7] Y. Shang, M. Brown, Molecular determinants for the tissue specificity of SERMs, *Science* 295 (2002) 2465–2468, <https://doi.org/10.1126/science.1068537>.
- [8] C.D. Runowicz, J.P. Costantino, D.L. Wickerham, R.S. Cecchini, W.M. Cronin, L. G. Ford, V.G. Vogel, N. Wolmark, Gynecologic conditions in participants in the NSABP breast cancer prevention study of tamoxifen and raloxifene (STAR), *Am. J. Obstet. Gynecol.* 205 (535) (2011) e1–5, <https://doi.org/10.1016/j.ajog.2011.06.067>.
- [9] S. Martino, D. Disch, S.A. Dowsett, C.A. Keech, J.L. Mershon, Safety assessment of raloxifene over eight years in a clinical trial setting, *Curr. Med. Res. Opin.* 21 (2005) 1441–1452, <https://doi.org/10.1185/030079905X61839>.
- [10] J. Ashby, J. Odum, J.R. Foster, Activity of raloxifene in immature and ovariectomized rat uterotrophic assays, *Regul. Toxicol. Pharm.* 25 (1997) 226–231, <https://doi.org/10.1006/rtp.1997.1108>.
- [11] S. Mirkin, D.F. Archer, H.S. Taylor, J.H. Pickar, B.S. Komm, Differential effects of menopausal therapies on the endometrium, *Menopause* 21 (2014) 899–908, <https://doi.org/10.1097/GME.0000000000000186>.
- [12] B.S. Komm, Y.P. Kharode, P.V.N. Bodine, H.A. Harris, C.P. Miller, C.R. Lyttle, Bazedoxifene acetate: A selective estrogen receptor modulator with improved selectivity, *Endocrinology* 146 (2005) 3999–4008, <https://doi.org/10.1210/en.2005-0030>.
- [13] D.W. Stovall, W.H. Utian, M.L.S. Gass, Y. Qu, D. Muram, M. Wong, L. Plouffe, The effects of combined raloxifene and oral estrogen on vasomotor symptoms and endometrial safety, *Menopause* 14 (2007) 510–517, <https://doi.org/10.1097/GME.0b013e318031a83d>.
- [14] A.M. Brzozowski, A.C. Pike, Z. Dauter, R.E. Hubbard, T. Bonn, O. Engström, L. Öhman, G.L. Greene, J.-A. Gustafsson, M. Carlquist, Molecular basis of agonism and antagonism in the estrogen receptor, *Nature* 389 (1997) 753–758, <https://doi.org/10.1038/39645>.
- [15] A.C. Pike, A.M. Brzozowski, R.E. Hubbard, T. Bonn, A.-G. Thorsell, O. Engström, J. Ljunggren, J.-A. Gustafsson, M. Carlquist, Structure of the ligand-binding domain of oestrogen receptor beta in the presence of a partial agonist and a full antagonist, *EMBO J.* 18 (1999) 4608–4618, <https://doi.org/10.1093/emboj/18.17.4608>.
- [16] A.C. Pike, A.M. Brzozowski, J. Walton, R.E. Hubbard, A.-G. Thorsell, Y.-L. Li, J.-A. Gustafsson, M. Carlquist, Structural insights into the mode of action of a pure antiestrogen, *Structure*. 9 (2001) 145–153, [https://doi.org/10.1016/S0969-2126\(01\)00568-8](https://doi.org/10.1016/S0969-2126(01)00568-8).
- [17] A.K. Shiau, D. Barstad, P.M. Loria, L. Cheng, P.J. Kushner, D.A. Agard, G.L. Greene, The structural basis of estrogen receptor/coactivator recognition and the antagonism of this interaction by tamoxifen, *Cell* 95 (1998) 927–937, [https://doi.org/10.1016/S0092-8674\(00\)81717-1](https://doi.org/10.1016/S0092-8674(00)81717-1).
- [18] Y.-L. Wu, X. Yang, Z. Ren, D.P. McDonnell, J.D. Norris, T.M. Willson, G.L. Greene, Structural basis for an unexpected mode of SERM-mediated ER antagonism, *Mol. Cell* 18 (2005) 413–424, <https://doi.org/10.1016/j.molcel.2005.04.014>.
- [19] J. Min, V.S. Guillen, A. Sharma, Y. Zhao, Y. Ziegler, P. Gong, C.G. Mayne, S. Srinivasan, S.H. Kim, K.E. Carlson, K.W. Nettles, B.S. Katzenellenbogen, J. A. Katzenellenbogen, Adamantyl antiestrogens with novel side chains reveal a spectrum of activities in suppressing estrogen receptor mediated activities in breast cancer cells, *J. Med. Chem.* 60 (2017) 6321–6336, <https://doi.org/10.1021/acs.jmedchem.7b00585>.
- [20] L. Wang, V.S. Guillen, N. Sharma, K. Flessa, J. Min, K.E. Carlson, W. Toy, S. Braqi, B.S. Katzenellenbogen, J.A. Katzenellenbogen, S. Chandarlapaty, A. Sharma, New class of selective estrogen receptor degraders (SERDs): expanding the toolbox of PROTAC degraders, *ACS Med. Chem. Lett.* 9 (2018) 803–808, <https://doi.org/10.1021/acsmchemlett.8b00106>.
- [21] C.D. Jones, M.G. Jevnikar, A.J. Pike, M.K. Peters, L.J. Black, A.R. Thompson, J. F. Falcone, J.A. Clemens, Antiestrogens. 2. Structure-activity studies in a series of 3-aryloxy-2-arylbenzo [b] thiophene derivatives leading to [6-hydroxy-2-(4-hydroxyphenyl) benzo [b] thien-3-yl]-[4-(2-(1-piperidinyl) ethoxy) phenyl] methanone hydrochloride (LY 156758), a remarkably effective estrogen antagonist with only minimal intrinsic estrogenicity, *J. Med. Chem.* 27 (1984) 1057–1066, <https://doi.org/10.1021/jm00374a021>.
- [22] D.A. Bradley, A.G. Godfrey, C.R. Schmid, Synergistic methodologies for the synthesis of 3-aryloxy-2-arylbenzo[b]thiophene-based selective estrogen receptor modulators. Two concise syntheses of raloxifene, *Tetrahedron Lett.* 40 (1999) 5155–5159, [https://doi.org/10.1016/S0040-4039\(99\)00955-7](https://doi.org/10.1016/S0040-4039(99)00955-7).
- [23] J.A. Dodge, C.D. Jones, T.M.L. Bourgeois, Preparation of 3-[4-(2-heterocyclolethoxy)benzoyl]-2-phenylbenzothiofenes for use in alleviating the symptoms of post-menopausal syndrome., *Eur. Pat. Appl.* (1996), 67pp. CODEN. EPXXDW EP 738725 A2 19961023 CAN 126: 7985 AN 1996: 740256 77, n.d.
- [24] P. Shinde, S. Shinde, A. Renge, G. Patil, A. Rode, R. Pawar, An efficient synthesis of raloxifene in ionic liquid: A green approach, *LOC.* 6 (2009) 8–10, <https://doi.org/10.2174/157017809787003133>.
- [25] A. Pandey, D.L. Volkots, J.M. Seroogy, J.W. Rose, J.-C. Yu, J.L. Lambing, A. Hutchaleelaha, S.J. Hollenbach, K. Abe, N.A. Giese, R.M. Scarborough, Identification of orally active, potent, and selective 4-piperazinylquinazolines as antagonists of the platelet-derived growth factor receptor tyrosine kinase family, *J. Med. Chem.* 45 (2002) 3772–3793, <https://doi.org/10.1021/jm02143r>.
- [26] N. Shiyeyoshi, H. Kenji, S. Hidetaka, H. Takashi, O. Hiroyuki, T. Takeshi, S. Shinobu, Process for producing 3,4-dihydroquinazoline-4-one derivatives, *PCT Int. Appl.* (2003), 101pp PIXXD2 WO 2003064399, CAN 139:164805, n.d.
- [27] F. Haviv, J.D. Ratajczyk, R.W. DeNet, F.A. Kerdesky, R.L. Walters, S.P. Schmidt, J. H. Holms, P.R. Young, G.W. Carter, 3-[1-(2-Benzoxazolyl)hydrazino]propanetrilene derivatives: inhibitors of immune complex induced inflammation, *J. Med. Chem.* 31 (1988) 1719–1728, <https://doi.org/10.1021/jm00117a010>.
- [28] S. Djogic, M. Halabalaki, X. Alexi, D. Njamen, Z.T. Fomum, M.N. Alexis, A.-L. Skaltsounis, Isoflavonoids from *Erythrina poeppigiana*: evaluation of their binding affinity for the Estrogen receptor, *J. Nat. Prod.* 72 (2009) 1603–1607, <https://doi.org/10.1021/np900271m>.
- [29] J.D. Chodera, D.L. Mobley, Entropy-enthalpy compensation: role and ramifications in biomolecular ligand recognition and design, *Annu. Rev. Biophys.* 42 (2013) 121–142, <https://doi.org/10.1146/annurev-biophys-083012-130318>.
- [30] N. Fokialakis, G. Lambrinidis, D.J. Mitsiou, N. Aligiannis, S. Mitakou, A.-L. Skaltsounis, H. Pratsinis, E. Mikros, M.N. Alexis, A new class of phytoestrogens: evaluation of the estrogenic activity of deoxybenzoinzins, *Chem. Biol.* 11 (2004) 397–406, <https://doi.org/10.1016/j.bmc.2012.03.012>.
- [31] N. Fokialakis, X. Alexi, N. Aligiannis, D. Siriani, A.K. Meligova, H. Pratsinis, S. Mitakou, M.N. Alexis, Ester and carbamate ester derivatives of Biochanin A: Synthesis and in vitro evaluation of estrogenic and antiproliferative activities, *Bioorg. Med. Chem.* 20 (2012) 2962–2970, <https://doi.org/10.1016/j.bmc.2012.03.012>.
- [32] M. Koufaki, E. Theodorou, X. Alexi, F. Nikoloudaki, M.N. Alexis, Synthesis of tropolone derivatives and evaluation of their in vitro neuroprotective activity, *Eur. J. Med. Chem.* 45 (2010) 1107–1112, <https://doi.org/10.1016/j.ejmech.2009.12.006>.
- [33] T. Laube, First crystal structure analysis of an aliphatic carbocation—stabilization of the 3,5,7-Trimethyl-1-adamantyl Cation by C-C hyperconjugation, *Angew. Chem. Int. Ed. Engl.* 25 (1986) 349–350, <https://doi.org/10.1002/anie.198603491>.